

Testing the effect of surface coatings on alkali atom polarization lifetimes

S. J. Seltzer,¹ D. M. Rampulla,² S. Rivillon-Amy,³ Y. J. Chabal,³ S. L. Bernasek,^{2,a)} and M. V. Romalis¹

¹*Department of Physics, Princeton University, Princeton, New Jersey 08544, USA*

²*Department of Chemistry, Princeton University, Princeton, New Jersey 08544, USA*

³*Laboratory for Surface Modification, Rutgers University, Piscataway, New Jersey 08854, USA*

(Received 29 May 2008; accepted 31 July 2008; published online 24 November 2008)

The evaluation of different surface coatings used in alkali metal atomic magnetometers is necessary for the improvement of sensitivity of these devices. A method to measure the polarization lifetime of alkali atoms in the region between substrates with different coatings was developed to determine the effectiveness of the coating at preserving alkali spin polarization as well as chemical compatibility and high-temperature stability. Multiple coatings can be compared under identical experimental conditions, using an experimental geometry that allows surface characterization before and after evaluation of the polarization lifetime. Multilayered, cross-linked octadecyltrichlorosilane films, alkyltrichlorosilane monolayers, and octadecylphosphonic acid monolayers were evaluated using this approach. © 2008 American Institute of Physics. [DOI: 10.1063/1.2985913]

I. INTRODUCTION

Antirelaxation surface coatings reduce the effects of spin relaxation at the walls of alkali vapor cells, allowing for significantly enhanced atomic spin polarization lifetimes. Coated cells have been used for atomic magnetometry,^{1–6} atomic clocks,^{7,8} magneto-optical traps,^{9–11} and slow light¹² and quantum memory experiments.¹³ To date, the most effective, widely used coating is paraffin, which allows an alkali atom to collide up to 10 000 times with the cell wall before depolarizing.^{14–16} However, paraffin typically melts at temperatures of about 60–80 °C and so cannot be used for applications such as high alkali vapor density spin-exchange relaxation-free (SERF) magnetometers,^{17,18} which must operate at higher temperatures. Various silane molecules have also been demonstrated^{9,19–21} to reduce surface relaxation rates; in particular, octadecyltrichlorosilane (OTS) has been shown to allow up to 2000 bounces on the surface before depolarization and to operate at higher temperatures than paraffin.⁶

When an alkali atom collides with the wall of a cell, it interacts with the surface for a brief period of time, during which it is subject to large local electric and magnetic fields, and its spin coherence with the other atoms in the cell may be lost. Wall collisions typically occur more frequently than other relaxation mechanisms (i.e., spin-exchange and spin-destruction collisions) and can completely dominate the lifetime of the atomic polarization. Surface coatings prevent direct interaction between the atoms and cell walls, and coatings with low polarizability, such as paraffin, feature significantly smaller local fields than the bare surface, allowing the atoms to bounce off a coated surface many times while maintaining their polarization.¹⁴ Surface relaxation is also suppressed in vapor cells filled with a buffer gas that slows diffusion of atoms to the walls, but coated cells without buffer gas have several advantages. Although coated cells

may still require a small amount of quenching gas to prevent radiation trapping,²² without a high-pressure buffer gas atoms are still free to move between different parts of the cell. Pump and probe laser beams, therefore, do not need to fill the entire cell and can be made small, since the atoms are likely to pass through each beam at least once during a polarization lifetime. In addition, depolarization due to magnetic field gradients is suppressed because the atoms effectively average the field over the entire cell volume.²³ Also, in the absence of pressure broadening due to buffer gas, the optical linewidths of atomic transitions are narrower, allowing for the use of less-powerful lasers and resulting in larger optical rotation signals.²⁴

Recent advances in alkali-metal magnetometry have achieved extremely high sensitivity by operating at high alkali atom density ($\sim 10^{13}$ – 10^{14} cm⁻³), requiring temperatures outside the effective operating range of paraffin ($T > 100$ °C for cesium, $T > 150$ °C for potassium). These include the SERF magnetometer^{17,18} with demonstrated sensitivity of 0.75 fT/√Hz (Ref. 25) for near-dc magnetic fields and a tunable radio-frequency magnetometer^{26,27} with demonstrated sensitivity of 0.24 fT/√Hz (Ref. 28) for fields in the range of several kilohertz to several megahertz. Both types of magnetometers have fundamental sensitivity below 0.01 fT/√Hz. Previous demonstrations of these high-density magnetometers have used uncoated cells filled with buffer gas because of the unavailability of high-quality surface coatings that can operate at these temperatures; therefore, the development of robust wall coatings that allow many bounces at high temperatures would benefit these applications.

In order to evaluate and develop effective coatings, a method is needed which allows comparison of multiple coatings under identical experimental conditions. This paper describes the development and use of an easily reusable alkali vapor cell for the purpose of testing multiple coatings for effectiveness and suitability for high-density atomic magnetometry. Previous experiments investigating the effectiveness

^{a)}Electronic mail: sberna@princeton.edu.

of coatings^{9,19–21,29} have used individual coated cells, whereas the use of a cell that can accommodate easily removable test surfaces allows for efficient testing of many different types of coatings under the same conditions. In the design described here, individual glass or silicon slides may be coated and then inserted into the reusable cell for testing. Flat slides can be coated more easily and uniformly than closed-geometry cells, and this geometry allows for additional surface characterization tests, such as infrared spectroscopy, atomic force microscopy, and x-ray photoelectron spectroscopy, to be conducted both before and after exposure to the alkali vapor.

II. EXPERIMENTAL

A. Alkali cell

The alkali cell is made of pyrex and consists of two parts, the main body and a lid, that are joined together by an *o*-ring flange held by a high-temperature nylon clamp. Apiezon-*H* vacuum grease is used to seal the *o*-ring flange, because of its high working temperature and chemical compatibility with potassium vapor. The coated slides are 2 in. by 1 in. and sit in a grooved pyrex tray that keeps them parallel and separated by approximately 5 mm. The cell includes an ampoule of potassium metal in a separate retort; a small amount of potassium is chased into the main body of the cell to act as the source of alkali vapor during the experiment. The cell has an input port, normally sealed with an *o* ring, used for connecting high purity nitrogen and helium. When the cell is open during loading and unloading samples, a flow of high purity nitrogen through the cell is maintained to reduce the flow of air into the cell. A thin layer of oxidation on the surface of the chased potassium droplets in the cell typically occurs during this procedure. After the cell is sealed, a fresh surface of potassium may be exposed by filling the cell with several hundred Torr of helium to prevent diffusion of alkali vapor to other areas of the cell and then melting the potassium droplets with a torch. While this procedure allows the same droplets of potassium to be used multiple times, the alkali vapor pressure becomes lower with each use due to contamination, until fresh potassium must be chased into the main chamber from the retort. Opening the cell in an inert environment inside a glovebox may prevent oxidation. The use of multiple samples in a single alkali vapor cell may allow the possibility of cross contamination of coatings by volatile alkali-coating reaction products, or by volatilization of the actual coatings at high test temperatures. The metal oxide, carbide, phosphide, or silicide products which may be formed are not likely to be volatile, however, minimizing this concern. Multiple samples of the same coating are examined at one time and then compared to separate loadings of the cell with different coatings to control for this possibility.

III. POLARIZATION LIFETIME MEASUREMENT

The effectiveness of the coatings in maintaining long polarization lifetimes is determined by performing a relaxation-in-the-dark measurement of the longitudinal spin polarization lifetime, T_1 .³⁰ The lifetime T_1 can be considered an upper limit to T_2 , the magnetometer linewidth, and is

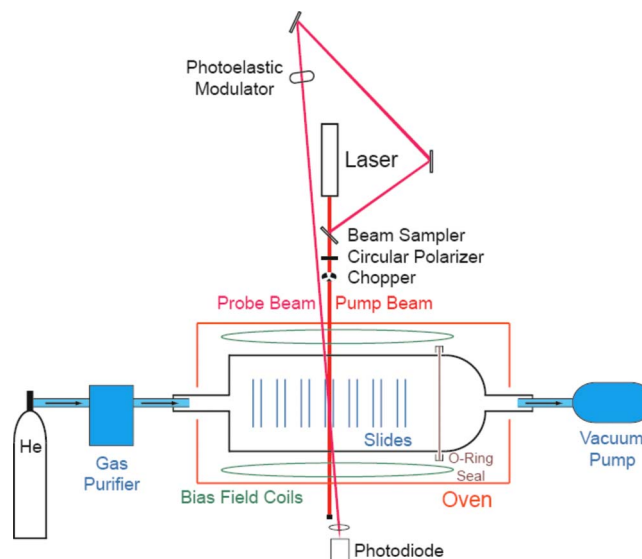


FIG. 1. (Color online) Setup of the polarization lifetime measurement. Nearly-parallel resonant pump and probe beams perform a relaxation-in-the-dark measurement of the polarization lifetime T_1 as pumping is modulated by an optical chopper. A supply of purified helium and a vacuum pump allow control of the buffer gas pressure in the cell.

equal to T_2 under some conditions (SERF magnetometer designs, for example). Field gradients can affect T_2 as well, and T_1 serves as a reasonable figure of merit of the effectiveness of the coating in increasing overall spin relaxation time. The setup of the experiment is shown in Fig. 1. An oven is used to heat the cell as high as 150 °C, though measurements are typically taken between 60 and 100 °C. The cell is connected to both high purity helium and a vacuum pump to allow for *in situ* control of the buffer gas pressure. The laser is a distributed feedback diode tuned to the $D1$ resonance of potassium at 770 nm. A small amount of laser light is picked off with a beam sampler to act as the probe beam; the polarization of this beam is modulated at approximately 50 kHz by a photoelastic modulator, and the transmission of light at this frequency is monitored by a photodiode and lock-in amplifier. The remaining laser light acts as the pump beam, is circularly polarized, expanded to fill the volume between two adjacent slides, and passed through an optical chopper. The paths of the two beams are kept at a small angle so that they intersect and are nearly parallel as they pass through the cell but diverge enough beyond the cell so that a photodiode detects only the probe beam. A pair of magnetic field coils creates a bias field of several Gauss along the direction of the laser beam to allow for efficient optical pumping.

When the chopper blocks the pump beam, the probe beam signal decays as shown in Fig. 2(a). After a brief period of time, typically a few milliseconds, the decay is dominated by the fundamental diffusion mode of the polarized atoms, and the data from the measurement are fitted to the sum of two decaying exponentials as shown in Fig. 2(b). The time constant of the first decaying exponential term is the polarization lifetime, T_1 , of the atoms due to the influence of the coated surfaces. The time constant of the second decaying exponential term is generally 5–10 times longer than that of the first term and represents the polarization lifetime in the

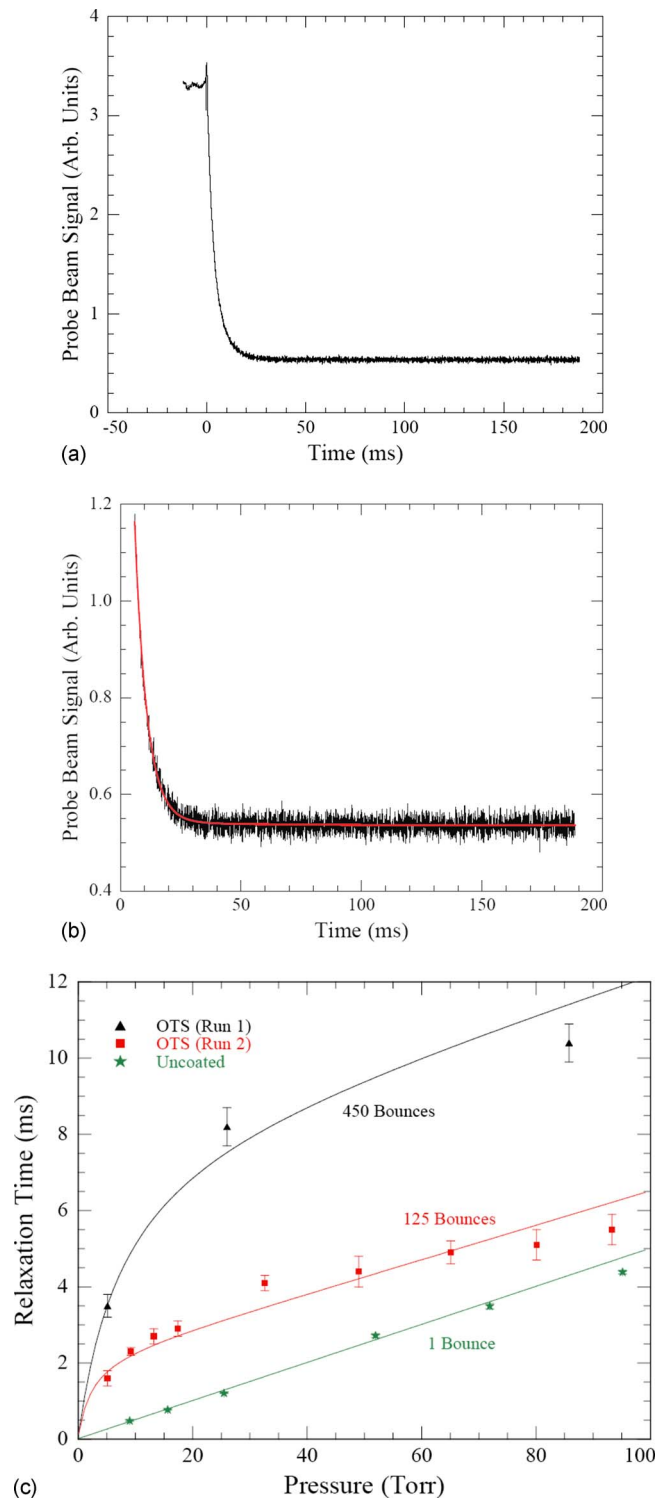


FIG. 2. (Color online) (a) Polarization data taken at 80 Torr of He that correspond to the data point along the 125 bounces curve shown in (c). (b) Enlarged portion of the data from (a) that shows the fitted curve (light gray, red online) of the sum of two decaying exponentials to extract T_1 . (c) Measurements of alkali polarization lifetimes as a function of buffer gas pressure, compared to values predicted by a mathematical model. The lifetime allowed by uncoated surfaces agrees with the model's prediction for a completely depolarizing surface, while measurements for thick, cross-linked OTS samples agree with predictions for surfaces allowing several hundred bounces.

absence of the surfaces; this time constant is measured far from the slides, and the relative weight (pre-exponential constant) of this term is significantly smaller than that of the first

term. The data shown in Figs. 2(a) and 2(b) give $T_1 = 5.1 \pm 0.2$ ms, and the y-axis offset is due to imperfection of the polarization of the probe beam. The measurement is repeated at different probe beam intensities to ensure that absorption of probe beam photons does not affect the measured polarization lifetime. The error in the lifetime measurement is determined by starting the data fit at successively later instances in time and noting the variation in the fit value for T_1 .

To prevent the potassium atoms from diffusing out of the region between the sample slides during the measurement, the cell is filled with helium buffer gas. Because the distance between slides is much smaller than the length of the slides along the other two dimensions, the polarization lifetime is dominated by diffusion along the dimension between the slides. The number of bounces, N , allowed by the coated surfaces can be determined from the measurement of T_1 as a function of buffer gas pressure, p . The theory of alkali depolarization at a coated surface in the presence of buffer gas is presented in Ref. 31. Briefly, the flux of polarized atoms to the surface, J_+ , and away from the surface, J_- , are given by:

$$J_+ = nv \left(\frac{1}{4} P - \frac{D(p)}{2v} \frac{\partial P}{\partial x} \right) \quad (1)$$

$$J_- = nv \left(\frac{1}{4} P + \frac{D(p)}{2v} \frac{\partial P}{\partial x} \right), \quad (2)$$

where \hat{x} is the dimension between the slides, P is the polarization of the atoms as a function of location and time, v is the thermal velocity of the atoms, n is the density of the alkali vapor, and $D(p)$ is the diffusion constant of alkali atoms as a function of buffer gas pressure. The probability of an atom depolarizing during a collision with the surface is $1/N$, so the reflected current of polarized atoms $J_- = (1 - 1/N)J_+$, and the gradient of polarization at the surface gives the boundary condition

$$\frac{\partial P}{\partial x} = \frac{-vP}{2N(2 - 1/N)D(p)}. \quad (3)$$

Along the other two dimensions the boundaries are defined by the openings out of the volume between the two slides, and the boundary conditions are similar to Eq. (3), except that $N \sim 1$ since polarized atoms diffusing out of this volume are generally lost to the measurement and replaced by unpolarized atoms diffusing into the volume.

The change of atomic polarization with time is described by the standard diffusion equation

$$\frac{\partial P}{\partial t} = D(p)\nabla^2 P - \Gamma_{SD}P, \quad (4)$$

where Γ_{SD} is the rate of spin-destruction collisions with buffer gas atoms and is a function of buffer gas pressure. The solution to Eq. (4) for the fundamental diffusion mode of the potassium atoms is

$$P = \cos(k_x x) \cos(k_y y) \cos(k_z z) e^{-t/T_1}, \quad (5)$$

where \vec{k} is the diffusion wave vector. Combining Eqs. (4) and (5) gives

$$\frac{1}{T_1} = D(p)(k_x^2 + k_y^2 + k_z^2) + \Gamma_{SD} \quad (6)$$

and applying the boundary condition (Eq. (3)) gives

$$k_x \tan\left(\frac{k_x L_x}{2}\right) = \frac{v}{2N(2 - 1/N)D(p)}$$

$$k_y \tan\left(\frac{k_y L_y}{2}\right) = \frac{v}{2D(p)}$$

$$k_z \tan\left(\frac{k_z L_z}{2}\right) = \frac{v}{2D(p)}, \quad (7)$$

where L_x is the distance between slides, and L_y and L_z are the length and height of the slides. Equations (6) and (7) can be combined and solved numerically for the polarization lifetime T_1 for a particular buffer gas pressure and relaxation efficiency of the test coating. Data collected from coated slides are shown in Fig. 2(c).

IV. RESULTS AND DISCUSSION

After the development of the alkali cell capable of accommodating interchangeable coated slides, the relationship between the structure and composition of organic surface coatings and their antirelaxation properties was examined. Initial efforts have focused on a variety of self-assembled monolayers (SAMs) coated on Si(100) wafers with 100 nm of a thermal oxide, as well as on borosilicate glass slides. These measurements serve as an example of the utility and effectiveness of this method to compare the antirelaxation properties of various organic coatings under the same conditions. SAMs are thin films of molecules (typically having a thickness consistent with the length of the constituent molecule) that are bound to the underlying substrate through a chemical bond. Eventually nonbonding interactions drive the molecules, often with long alkyl chains, to align with each other in a vertical orientation, and this two-dimensional (2D) aggregation continues until the available binding sites are filled. SAMs were chosen because they produce an ordered and homogeneous array of molecules, which are conducive to surface studies. IR spectroscopy was used to verify the order and homogeneity of the SAMs before and after exposure to K vapor. Relaxation time (T_1) was measured in the alkali vapor cell to test the effectiveness of the coatings to inhibit spin relaxation after exposure to K vapor and changes in temperature. Although this is not a comprehensive investigation of the relationship between T_1 and the structure and composition of SAMs, this study offers an initial effort toward understanding the surface relaxation processes of alkali atoms. Butylchlorosilane [BTS, $\text{CH}_3(\text{CH}_2)_3\text{SiCl}_3$], dodecyltrichlorosilane [DTS, $\text{CH}_3(\text{CH}_2)_{11}\text{SiCl}_3$], and octadecyltrichlorosilane [OTS, $\text{CH}_3(\text{CH}_2)_{17}\text{SiCl}_3$] monolayers on Si(100) wafers were examined. Thicker, cross-linked OTS films were also grown on Si(100) wafers. Finally, octadecylphosphonic acid [ODPA, $\text{CH}_3(\text{CH}_2)_{17}\text{P}(\text{OH})_2\text{O}$] monolayers on Si(100) wafers and glass slides were studied. These organic molecules were chosen because their long hydrocarbon chains resemble those found in paraffin films.

BTS, DTS, and OTS monolayers were grown on rectangular Si(100) samples that were cleaned using the RCA standard cleaning procedure (SC-1/SC-2). They are first immersed in a hydrogen peroxide (H_2O_2)/ammonium hydroxide (NH_4OH)/de-ionized water (DIW, 18.2 M Ω cm) solution (1:1:4 v/v) (SC-1), and then in a H_2O_2 /hydrochloric acid (HCl)/DIW solution (1:1:4) (SC-2). Both treatments are performed at 80 °C for 10 min, and the Si(100) samples are thoroughly rinsed with DIW between each step and finally dried under nitrogen gas (N_2) flow. After cleaning each sample, they are immediately introduced into a N_2 -purged glovebox for further functionalization with silane-based molecules. Anhydrous toluene, BTS, DTS, and OTS are purchased from Sigma Aldrich and used without further purification. After placing in the N_2 -purged glovebox, the cleaned Si(100) samples are immersed in a freshly prepared solution of either BTS, DTS, or OTS (0.1 vol %) in anhydrous toluene. During the 48 h reaction, the reaction tube is sealed to avoid any additional contamination. The reaction takes place at room temperature. After completion, the sample is removed from the solution, rinsed thoroughly with anhydrous toluene, and immersed in a fresh solution of anhydrous toluene in order to be removed from the glovebox. The samples are then sonicated for 5 min and finally dried under a stream of N_2 . This procedure ensures that the silane molecules are bound to the underlying substrate through all available ligands, thus cross-linking is kept to a minimum.

The procedure for coating thick, cross-linked films of OTS has been adapted from previous work.^{32,33} The slides were cleaned with piranha solution consisting of three parts hydrogen peroxide to seven parts sulfuric acid by volume. The solution was allowed to cool down for 1 h prior to use. The Si(100) slides were submerged in the piranha solution for 1 h, removed, rinsed three times with DIW, and then rinsed three times with methanol. The cleaning steps occurred in a fume hood, which exposed all of the slides and solutions to ambient conditions. After cleaning, the slides were transferred to a vacuum oven and baked at 150 °C for 1 h. Afterward, the samples were returned to the fume hood for OTS coating. A solution of one part chloroform to four parts hexanes was made, and OTS was added to the solution such that its concentration was 0.8 mL OTS/1 L of solution. The slides were exposed to the OTS solution for 5 min and then exposed to ambient air for 5 min. The slides were then rinsed three times with chloroform and then transferred to the vacuum oven to be baked at 200 °C for 24 h. The OTS coatings made using this procedure were determined to be ~4.9 nm (~2 layers) thick by using angle-resolved x-ray photoelectron spectroscopy.³⁴ The films were not formed in a dry and inert environment similar to the other alkylsilane monolayers, and the presence of an ambient environment leads to a high-degree of cross-linking and thicker films. It is important to note that we have not verified cross-linking in these OTS films, but the procedure used is conducive to the formation of cross-linked films.

The procedure for coating monolayers of ODPA has been explained in detail elsewhere.³⁵ The ODPA coating procedure was repeated one (80% coverage), two (90% cover-

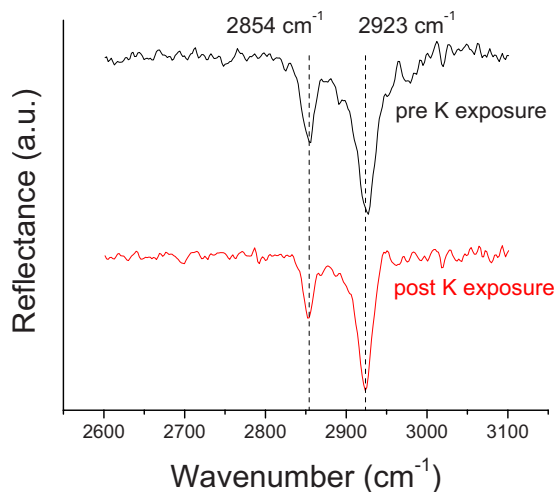


FIG. 3. (Color online) IR spectroscopy of an OTS monolayer. Indicating the presence of a well-ordered monolayer, DTS and OTS monolayers exhibited similar spectral features at ~ 2920 cm^{-1} (asymmetric C-H vibrational mode) and ~ 2850 cm^{-1} (symmetric C-H vibrational mode). The minimal changes in spectral features upon exposure of the film to *K* vapor indicate that the film remains intact.

age), and three ($>90\%$ coverage) times on various samples to ensure a high coverage of the monolayers.³⁵

Before exposing the silane monolayers to *K* vapor, IR spectroscopy was performed to establish film order. DTS and OTS were observed to be well-ordered monolayers, due to the presence of intense absorbance peaks at ~ 2920 cm^{-1} (asymmetric C-H vibrational mode) and ~ 2850 cm^{-1} (symmetric C-H vibrational mode) as shown in Fig. 3. Broad absorbance peaks and peaks that are shifted from the standard values are indicative of a disordered monolayer. BTS monolayers could not be characterized by IR spectroscopy, because there are too few C-H bonds present on the surface to adequately detect any absorbance.

Measurements of T_1 were carried out in the presence of these organic layers, and the results are presented below. The BTS film gave a measured $T_1 = 1.1 \pm 0.1$ ms (at 10 Torr He) in the temperature range of 65–145 °C, which was greater than the, $T_{1,\text{bare}} = 0.5 \pm 0.1$ ms measured for the bare Si wafer at this pressure. Although $T_{1,\text{BTS}}$ was static throughout the temperature range, $T_{1,\text{DTS}}$ exhibited a clear and surprising temperature dependence, beyond temperature effects on the diffusion constant of the alkali atoms. Figure 4 shows the reversible temperature dependence observed for $T_{1,\text{DTS}}$ between 65 and 95 °C. $T_{1,\text{DTS}} = 2.3 \pm 0.1$ ms (at 10 Torr He) at 65 °C, but at 95 °C, $T_{1,\text{DTS}}$ dropped to 1.2 ± 0.1 ms (at 10 Torr He). Upon cooling to 65 °C, $T_{1,\text{DTS}}$ increased to 2.0 ± 0.1 ms, which was close to the original value. Repeated heating and cooling cycles produced the observed decrease and increase in $T_{1,\text{DTS}}$, yet the relaxation time never fully recovered to its original value of 2.3 ms. When compared to the other silane monolayers, the OTS monolayers demonstrated a low relaxation time, $T_1 = 0.9 \pm 0.1$ ms (at 10 Torr He), between 65 and 95 °C. Contrary to what was observed with DTS, no T_1 temperature dependence was seen with OTS. After exposure to *K* vapor, IR spectroscopy confirmed that the DTS and OTS monolayers remained intact, which was expected, since T_1 measurements for all silanes

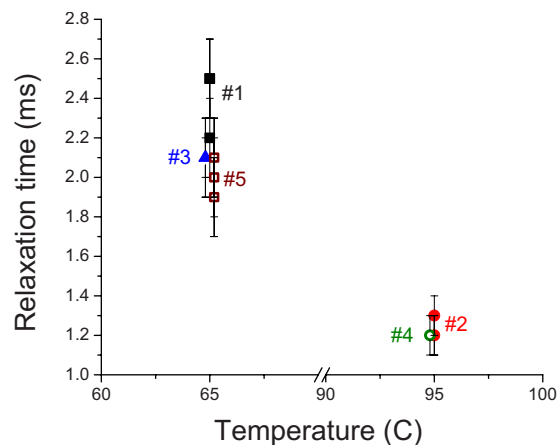


FIG. 4. (Color online) Reversible temperature dependence of $T_{1,\text{DTS}}$. Data 1 is the first measurement at 65 °C, data 2 is at 95 °C, data 3 is cooling to 65 °C, and data 4 and 5 subsequent heating and cooling to 95 and 65 °C. Individual data points in each numbered group are repeated measurements with the indicated temperature held constant.

remained above the bare Si limit of 0.5 ms. The only change seen with IR spectroscopy was the narrowing of spectral features. Figure 3 shows the pre-*K* and post-*K* exposure IR spectra. In the pre-*K* exposure spectrum the peak at ~ 2920 cm^{-1} had a Full Width at Half Maximum (FWHM) of 30.3 cm^{-1} , but the same peak in the post-*K* exposure spectrum had a FWHM of 21.0 cm^{-1} . The narrowing indicates an increase in monolayer order,^{36,37} which was likely due to the thermal annealing experienced at temperatures up to 95 °C.

The antirelaxation behavior of the thick, cross-linked OTS layer is shown in Fig. 2. The cross-linked OTS sample displayed a $T_1 = 3.5 \pm 0.1$ ms (Run 1), and at a later time the same surface exhibited a $T_1 = 1.5 \pm 0.1$ ms (Run 2) at temperatures of 70 °C (at 5 Torr He), possibly due to condensation of potassium on the slides. The time between the two runs was 48 h, and it is clear that the cross-linked OTS films changed with time under a constant temperature and *K* exposure. By systematically increasing the He pressure in the test cell, T_1 versus p was plotted and the approximate number of bounces was extracted. The first run of the cross-linked OTS samples showed 450 bounces until depolarization, and the second run for this sample (48 h later) showed 125 bounces. For comparison, uncoated samples displayed much shorter relaxation times consistent with a single bounce.

IR spectroscopy of the pre-exposed ODP A monolayers showed well-ordered monolayers that were similar to DTS and OTS; however, after exposure to *K* vapor, IR spectroscopy showed no evidence of any C-H vibrational modes on the surface. For *all* ODP A films, relaxation time measurements at 55 °C (at 10 Torr He) were $T_{1,\text{ODPA}} = 0.5 \pm 0.1$ ms, which is comparable to the relaxation time for bare Si and glass surfaces. Relaxation time measurements corroborate the notion that the film is damaged (or destroyed) in the presence of *K* vapor and does not function as an antirelaxation coating.

Although inferior to paraffin, all silane monolayer coatings were shown to possess antirelaxation properties. All si-

lane monolayers were capable of sustaining antirelaxation properties at higher temperatures; however, evidence shows that antirelaxation efficacy decreases with an increase in temperature for DTS monolayers. This is the first instance in which antirelaxation properties have been related to temperature of the film, except when the film melts or decomposes above some critical temperature. Since the change in $T_{1,DTS}$ is reversible and temperature dependent, we speculate that the film experiences a phase change at higher temperatures, such as a reordering of the SAM molecules, which could lead to exposure of larger patches of the bare, depolarizing substrate. Because IR spectroscopy indicated that DTS and OTS were both well-ordered films, it is not known why $T_{1,OTS}$ did not have a similar temperature dependence as that seen for $T_{1,DTS}$.

The highest T_1 measured in this study was from the first run of thick, cross-linked OTS films. There are two primary differences between the OTS monolayers with a $T_1 = 0.9$ ms (at 10 Torr He), equivalent to approximately 25 bounces, and the OTS films with a $T_1 = 5$ ms (at 10 Torr He), equivalent to approximately 450 bounces. First, angle-resolved x-ray photoelectron spectroscopy showed that the thickness of the multilayer OTS film is approximately twice the thickness of the OTS monolayer. The second difference is the possible presence of cross-linking in the thicker film. This cross-linking could lead to a stiffer film, some structural change, or just a simple reduction in the number of available oxygen atoms in the film. Regardless of the underlying physical or chemical difference, it is clear that the antirelaxation abilities of the two OTS films are drastically different. It should be noted that the same procedure used to coat these samples with thicker films was used to coat a glass magnetometer cell that achieved ~ 2000 bounces until alkali depolarization.⁶ Although the 450 bounces observed for this film is lower than what is possible with this coating, the results are comparable to the other cells described in Ref. 6.

Finally, $T_{1,ODPA}$ was comparable to T_1 on bare glass or Si wafers, thus the alkali atoms experienced a completely depolarizing interaction. It should be noted that ODPA has been shown to remain intact on oxide surfaces up to 140 °C (Ref. 35); therefore, it is not likely that the monolayer degraded due to thermal annealing. Although the precise reaction mechanism between K atoms and the ODPA monolayers is unknown, it is clear that the monolayer has been significantly degraded by the presence of K vapor. Even the best prepared (triple-coated monolayer) films show decomposition. Previous work with metal vapors (Al, Cu, Ag, Au) shows that metal atoms may penetrate SAMs,³⁸ and we expect K to behave similarly. The areal density of a well-ordered ODPA monolayer is 18.5 Å²/molecule,³⁵ which translates into a chain-to-chain separation of 4.3 Å, the value expected for close-packed aliphatic chains.³⁹ At this chain separation, K atoms may be able to penetrate even well-ordered SAMs, and if so, they should easily penetrate the film at defect sites and domain boundaries. If K atoms are able to penetrate, then bonding groups that attach the organic monolayer to the substrate could react with the alkali atoms, resulting in film

degradation. Based on the behavior of the ODPA versus OTS films, perhaps phosphonate groups are more reactive to K atoms than silane groups.

V. CONCLUSIONS

The primary purpose of this work was to develop an alkali test cell that allows for rapid testing of antirelaxation properties of surface coatings on flat substrates, allowing for ease of subsequent studies of surface composition and structure to understand surface contributions to alkali atom relaxation mechanisms. To this end, we measured relaxation times for various SAMs, thus showing that the test cell is suitable for its intended use. Additionally, a previously undocumented, reversible change in antirelaxation quality as a function of temperature was observed for a DTS monolayer. Now that the alkali test cell is functional, further studies are underway to extract the relationship between alkali depolarization and surface properties, such as thickness, stiffness, order/disorder, substrate roughness, potential energy corrugation, and chemical composition. This understanding will hopefully lead to the development of high-quality surface coatings for alkali vapor cells operating at high temperatures.

ACKNOWLEDGMENTS

This work was supported by an Office of Naval Research MURI Grant No. SA4845-10556. The authors thank Dima Budker, Jeffrey Schwartz, Joe Dennes, and Amber Hibberd for helpful discussions, and Ken Andreas and Mike Souza for help in the construction of the alkali cell.

- ¹S. Groeger, A. S. Pazgalev, and A. Weis, *Appl. Phys. B: Lasers Opt.* **80**, 645 (2005).
- ²P. D. D. Schwindt, L. Hollberg, and J. Kitching, *Rev. Sci. Instrum.* **76**, 126103 (2005).
- ³S. Groeger, G. Bison, J.-L. Schenker, R. Wynards, and A. Weis, *Eur. Phys. J. D* **38**, 239 (2006).
- ⁴M. V. Balabas, D. Budker, J. Kitching, P. D. D. Schwindt, and J. E. Stalnaker, *J. Opt. Soc. Am. B* **23**, 1001 (2006).
- ⁵M. P. Ledbetter, V. M. Acosta, S. M. Rochester, D. Budker, S. Pustelny, and V. V. Yashchuk, *Phys. Rev. A* **75**, 023405 (2007).
- ⁶S. J. Seltzer, P. J. Meares, and M. V. Romalis, *Phys. Rev. A* **75**, 051407 (2007).
- ⁷D. Budker, L. Hollberg, D. F. Kimball, J. Kitching, S. Pustelny, and V. V. Yashchuk, *Phys. Rev. A* **71**, 012903 (2005).
- ⁸J. S. Guzman, A. Wojciechowski, J. E. Stalnaker, K. Tsigtukin, V. V. Yashchuk, and D. Budker, *Phys. Rev. A* **74**, 053415 (2006).
- ⁹M. Stephens, R. Rhodes, and C. Wieman, *J. Appl. Phys.* **76**, 3479 (1994).
- ¹⁰Z.-T. Lu, K. L. Corwin, K. R. Vogel, C. E. Wieman, T. P. Dinneen, J. Maddi, and H. Gould, *Phys. Rev. Lett.* **79**, 994 LP (1997).
- ¹¹S. Aubin, E. Gomez, L. A. Orozco, and G. D. Sprouse, *Rev. Sci. Instrum.* **74**, 4342 (2003).
- ¹²M. Klein, I. Novikova, D. F. Phillips, and R. L. Walsworth, *J. Mod. Opt.* **53**, 2583 (2006).
- ¹³B. Julsgaard, J. Sherson, J. I. Cirac, J. Flurásek, and E. S. Polzik, *Nature (London)* **432**, 482 (2004).
- ¹⁴M. A. Bouchiat and J. Brossel, *Phys. Rev.* **147**, 41 (1966).
- ¹⁵H. G. Robinson and C. E. Johnson, *Appl. Phys. Lett.* **40**, 771 (1982).
- ¹⁶M. T. Graf, D. F. Kimball, S. M. Rochester, K. Kerner, C. Wong, D. Budker, E. B. Alexandrov, M. V. Balabas, and V. V. Yashchuk, *Phys. Rev. A* **72**, 023401 (2005).
- ¹⁷J. C. Allred, R. N. Lyman, T. W. Kornack, and M. V. Romalis, *Phys. Rev. Lett.* **89**, 130801 (2002).
- ¹⁸I. K. Kominis, T. W. Kornack, J. C. Allred, and M. V. Romalis, *Nature (London)* **422**, 596 (2003).
- ¹⁹J. C. Camparo, *J. Chem. Phys.* **86**, 1533 (1987).

- ²⁰D. R. Swenson and L. W. Anderson, *Nucl. Instrum. Methods Phys. Res. B* **29**, 627 (1988).
- ²¹J. A. Fedchak, P. Cabauy, W. J. Cummings, C. E. Jones, and R. S. Kowalczyk, *Nucl. Instrum. Methods Phys. Res. A* **391**, 405 (1997).
- ²²F. A. Franz, *Phys. Lett. A* **27**, 457 (1968).
- ²³G. D. Cates, S. R. Schaefer, and W. Happer, *Phys. Rev. A* **37**, 2877 (1988).
- ²⁴S. J. Seltzer and M. V. Romalis (unpublished).
- ²⁵T. W. Kornack, S. J. Smullin, S.-K. Lee, and M. V. Romalis, *Appl. Phys. Lett.* **90**, 223501 (2007).
- ²⁶I. M. Savukov, S. J. Seltzer, M. V. Romalis, and K. L. Sauer, *Phys. Rev. Lett.* **95**, 063004 (2005).
- ²⁷I. M. Savukov, S. J. Seltzer, and M. V. Romalis, *J. Magn. Reson.* **185**, 214 (2007).
- ²⁸S.-K. Lee, K. L. Sauer, S. J. Seltzer, O. Alem, and M. V. Romalis, *Appl. Phys. Lett.* **89**, 214106 (2006).
- ²⁹K. Zhao and Z. Wu, *Phys. Rev. A* **71**, 012902 (2005).
- ³⁰W. Franzen, *Phys. Rev.* **115**, 850 (1959).
- ³¹F. Masnou-Seews and M. A. Bouchiat, *J. Phys. (Paris)* **28**, 406 (1967).
- ³²M. S. Rosen, T. E. Chupp, K. P. Coulter, R. C. Welsh, and S. D. Swanson, *Rev. Sci. Instrum.* **70**, 1546 (1999).
- ³³D. C. Bear, "Fundamental symmetry tests using a $^{129}\text{Xe}/^3\text{He}$ dual noble gas maser," Ph.D. thesis, Harvard University, 2000.
- ³⁴D. M. Rampulla, N. Oncel, E. Abelev, and S. Bernasek (submitted).
- ³⁵E. L. Hanson, J. Schwartz, B. Nickel, N. Koch, and M. F. Danisman, *J. Am. Chem. Soc.* **125**, 16074 (2003).
- ³⁶R. G. Snyder, S. L. Hsu, and S. Krimm, *Spectrochim. Acta, Part A* **34**, 395 (1978).
- ³⁷N. V. Venkataraman and S. Vasudevan, *J. Phys. Chem. B* **106**, 7766 (2002).
- ³⁸A. V. Walker, T. B. Tighe, O. M. Cabarcos, M. D. Reinard, B. C. Haynie, S. Uppili, N. Winograd, and D. L. Allara, *J. Am. Chem. Soc.* **126**, 3954 (2004).
- ³⁹A. I. Kitaigorodskii, *Organic Chemical Crystallography* (Consultants Bureau, New York, 1961).